Original Article
Application of magnetic resonance spectroscopy in the preoperative grading of gliomas

Xiao Shen[1], Ersong Wang[1], Chengjun Yao[2], Weijun Tang[3], Jun Guo[4]

[1]Department of Neurosurgery, Jinshan Hospital, Fudan University, Shanghai 200433, China; Departments of [2]Neurosurgery, [3]Radiology, Huashan Hospital, Fudan University, Shanghai 200433, China; [4]Department of Neurosurgery, The First People's Hospital of Yancheng, Jiangsu, China

Abstract: This study aims to assess Proton Magnetic Resonance Spectroscopy (1H-MRS) for diagnosis and preoperative grading of cerebral gliomas. A multi point biopsy under 1H-MRS metabolism imaging guidance in 21 cerebral glioma patients was performed preoperatively to obtain the corresponding voxel tissue samples. The gliomas were graded according to MRS and results compared with routine MRI and pathology data, respectively. One hundred and sixteen tissue samples were obtained by biopsy, and the puncture target exactly matched the selected voxel. Choline/N-acetyl aspartate (Cho/NAA) ratios positively correlated with pathological grades (r=0.368, P=0.031). The Cho/NAA ratio was 2.52 with a maximum Youden index of 0.7; based on these results, MRS had 92.9% sensitivity, 71.4% specificity, and 85.7% accuracy, and was more favorable than routine plain and enhanced MRI with 64.3% sensitivity, 85.7% specificity, and 71.4% diagnosis accordance (P=0.040). MRS may contribute to accuracy improvement for grading cerebral gliomas prior to operation.

Keywords: Proton magnetic resonance spectroscopy, neuronavigation, biopsy, glioma, brain tumors

Introduction

Glioma is the most common central nervous system malignancy and arouses a great concern due to its high invasiveness, mortality and recurrence [1]. Considering the diversity in treatment and diagnosis different grades in approaches for gliomas, accurate grading is of great importance to verify prognosis and initiate the most appropriate treatment strategy for patients with gliomas. Currently, tissue samples are generally obtained by surgical resection or stereotactic biopsy and are subsequently graded pathologically; this is usually limited by grading inaccuracy with partial resection of the tumor or inappropriate biopsy specimens [2, 3]. Edward et al. [4-6] explained unconfirmed pathological diagnosis or misdiagnosis as follows: (1) traditional operation is based on the anatomical structure from MRI data, which reflect the tumor-induced destruction of the blood-brain barrier, and may result in false negatives; (2) confirming the lesions with highest malignancy is critically important due to the heterogeneity of tumor metabolism, since it

may be misdiagnosed if the specimen is limited by a biopsy. Accordingly, a new approach is required for tumor grading.

The choline/N-acetyl aspartate (Cho/NAA) ratio, which comprehensively reflects the changes of compound content of tumor volume, always increases with malignancy and is quite sensitive in glioma grading. 1H-MRS can detect the metabolism imaging of lesions by measuring the concentration alteration of particular organization metabolites and Cho/NAA, providing a new approach for the diagnosis and grading of glioma preoperatively. The current study aimed to determine an appropriate Cho/NAA value by analyzing the association between MRS and pathological grades of gliomas.

Materials and methods

Patient selection

This study was approved by the ethics committee of Huashan Hospital, Fudan University. From September 2010 to October 2011, twen-

Table 1. Location, pathology classification and grades of 21 selected gliomas

	Baseline data
Age	48.8 ± 13.2
Sex (male/female)	15/6
Location	
Left frontal lobe	4
Right frontal lobe	8
Right temporal occipital lobe	2
Left parietal lobe	2
Right parietal lobe	1
Bilateral parietal lobe	1
Left insula	1
Left basal ganglia	1
Right thalamus	1
Pathology classification	
Astrocytoma	4
Oligodendroglioma	4
Anaplastic astrocytoma	5
Glioblastoma	8
Grade (WHO)	
II	7
III	6
IV	8

ty-one patients with brain tumors and MRI confirmed lesion locations but unconfirmed properties were later diagnosed with glioma by pathology postoperatively and retrospectively analyzed. There were 15 males and 6 females aged between 16 and 71 years (mean age of 48.8 ± 13.2 years); lesion volumes ranged from 24 to 62.3 cm^3 (40.2 ± 7.8 cm^3). The percentages of patients with lassitude, lethargy/headache and speech dysfunction were 61.9% (13/21), 39.1% (8/21) and 28.6% (6/21), respectively. All participants provided written informed consent. The glioma details are displayed in **Table 1**.

Equipment and parameters

Surgical system: a comprehensive operating center system was used in this study, including an operating and diagnosis room (IMRIS Inc., Canada), a 3.0T MAGNETOM Verio MR system (Siemens Healthcare, Siemens AG, Germany), a Stealth Station TRIA i7 Neuronavigation system (Medtronic Navigation Inc., America), and an Image post-processing workstation (Syngo Multi Modality Workplace, Siemens Healthcare,

Siemens AG, Germany). The puncture appliance was Navigus System for Frameless Access (Medtronic Navigation Inc., USA).

Magnetic resonance imaging (MRI)

MRI T1 weighted images (TR/TE, 600/16 ms) and T2 weighted images (TR/TE, 5100/138 ms) were obtained using spin echo (SE) and fast spin echo (FSE) sequences; T1 and T2 slice thicknesses were 5-8 mm with the slice gap 1.5 mm. The complete scanning was performed in three slices. On the basis of T1 weighted images of SE sequences, MR enhanced scan images were obtained. The following indicators needed to be noted in the MRI plain scan and enhanced: (1) the situation of tumor texture and necrosis; (2) presence or absence of bleeding; (3) presence or absence of space occupying effect; (4) presence or absence of blood brain barrier damage. According to the subjective judgment of surgeons and radiologists, the cases were diagnosed as low or high grade glioma based on the status of uneven texture, necrosis, hemorrhage, occupying effect, and enhancement of tumors through MRI evaluation.

Pointed-resolved spectroscopy sequence of three dimensional multi-voxel was used in MRS, usually with the metabolites NAA, Cho, Cr, and Lip (TR/TE=1000 ms/144 ms). The voxel thickness was 10 mm with the slice gap of 2 mm. The size of field of view (FOV) depended on the lesion condition, including region of tumor enhancement, tumor edema, and normal brain tissue away from the lesion. The phasic matrix was 160×160 mm and the size of region of interest (ROI) varied from 0.5×0.5×0.5 cm^3 to 1×1×1 cm^3.

The ROI contained glioma enhanced area, abnormal signal area and surrounding region of tumor, and normal brain tissue can be selected as control if necessary; in addition, the selected voxel is usually in a straight line, which is convenient for needle biopsy.

Fusion of MRS metabolic imaging and 3D navigation imaging

All data transmitted through the local area network to the image post-processing workstation were used to automatically calculate Cho/NAA ratios with the software Spectroscopy (Syngo

Multi Modality Workplace, Siemens Healthcare, Siemens AG, Germany) on the nuclear magnetic resonance system. The area with high Cho/NAA was selected to design the preoperative piercing trajectory and target. Notably, the piercing trajectory should avoid the conduction bundle and functional region as much as possible. Osirix (v.3.7.1 32-bit version, Apple Inc., USA) was used to import and read images, and record all the voxel coordinates of targets (X, Y, Z). Running in the Matlab (7.7.0 version, Mathworks Inc., America) environment, the original spectra, neuronavigation data, and voxel coordinates of biopsy targets were orderly imported to the Biopsy-NAV software, which was developed by our study group and yields a more accurate biopsy position which confirms the MRI or MRS exam (i.e. ROI). The biopsy target's anatomic position, automatically marked in the navigation data, was then imported to the nerve navigation system, generating a fusion of MRS metabolic imaging and 3D anatomical imaging through post-processing by the workstation.

Biopsy NAV software

Biopsy NAV was designed by our study group, and was used for marking the MRS and MR image fusion. Since the data processed by the Spectroscopy software can only generate MRS 2D pixel maps with BMP format which are not directly useful for DICOM format navigation, a reasonable puncturing track must be set by MRS pseudo color pictures to record the voxel coordinates of interest (X, Y, Z); then, Biopsy NAV was started to convert the DICOM format data to NII. GZ format files, which were reconverted to DICOM format according to the mark set by the corresponding coordinate of different voxel coordinates of interest. Namely, the voxel coordinates of interest in MRS were marked and fused with structure imaging navigation through the segmentation and reassembly of imaging data, and ultimately transmitted to the navigation system.

Sampling under navigation

To obtain the one-to-one correspondence between preselected voxel and biopsy specimen, all cases underwent a needle biopsy prior to craniotomy. The puncture base was fixed following the sphenotresia, and the needle direction was adjusted and fixed. The accurate punc-

ture matching between voxel and biopsy specimen was guaranteed under the navigation. According to the preoperative design, each specimen was sampled in four directions to make the location and size coincide with the corresponding voxel, subsequently, the puncture needle was retentive to stop bleeding for several minutes. The intraoperative MRI scanning for the biopsy specimen was conducted to estimate the accuracy of puncture targets (the distance between the puncture targets and preselected voxel center was the puncture error when the iMRI imaging after needle puncture was fused with that of MRI prior to operation). To eliminate complications such as bleeding, the hematoma was cleared immediately with bleeding beyond 30 ml.

Pathological examination

All biopsy specimens fixed with 4% formaldehyde were sent to pathology department, where they were paraffin embedded, sectioned, stained with hematoxylin and detected by immunohistochemistry (EnVision). Diagnosis with H&E and immunohistochemical staining was confirmed by two neuropathology specialists according to the fourth edition of "WHO tumors of the central nervous system" published in 2007. Any discrepancy between two specialists was resolved by discussion and consultation with two additional neuropathology specialists.

Statistical analysis

All the statistical analyses were performed using SPSS 13.0 (Chicago, IL, USA). Receiver operating characteristic (ROC) curves were plotted, area under the curve (AUC) values was calculated, sensitivity and specificity was determined, and correlation analysis was performed. Comparisons among groups were executed by Wilcoxon rank sum test. $P < 0.05$ was considered to be statistically significant.

Results

Functional imaging

The routine structure imaging of both MRI and MRS was obtained with stable spectral baselines and apparently increased Cho values and decreased NAA amounts in the concerned areas.

Table 2. Pathological grades of biopsy specimens and postoperative pathology data

Biopsy judgment	Pathological grade		
	II	III	IV
Cancer-free	6	2	1
II	23	13	7
III		27	20
IV			17

Table 3. Diagnoses by pathology, MRS and routine MRI

Pathological diagnosis	Routine MRI diagnosis		MRS diagnosis		Total
	High grade	Low grade	High grade	Low grade	
High grade	9	5	13	1	14
Low grade	1	6	2	5	7
Total	10	11	15	6	21
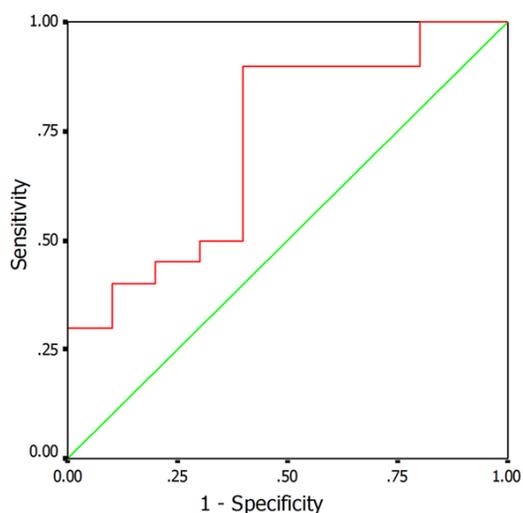
Figure 1. ROC curve of the Cho/NAA value for tumor tissue.

Pathology diagnosis

One hundred and sixteen tissue samples were obtained from 21 patients with cerebral glioma by biopsy, and puncture targets were exactly matched to the selected voxels with a deviation from the target averaging 0.5 ± 0.45 mm. Using pathological examination as gold standard, grades I and II gliomas were considered to be low grade, and grades III and IV were categorized as high grade. A total of 7 cases were diagnosed as low grade (7/21, 33%), and

14 as high grade (14/21, 67%) accordingly. Discrepancy between biopsy pathology results and postoperative pathology data was shown in **Table 2**.

A small amount of bleeding at puncture site was found on iMRI imaging in 1 patient after puncture, and craniotomy was immediately performed. The contralateral myodynamia of this patient decreased after operation, but recovered after two months. No new dysneuria was found in the remaining cases. Also, no death or infection after operation was found in the participants.

Comparison between MRS and routine MRI

Eleven and ten cases were diagnosed as low and high grade gliomas, by conventional MRI scan; meanwhile, six and fifteen cases were attributed to low and high grade gliomas by MRS according to the ROC results (showed below). Importantly, pathological diagnosis confirmed 7 low and 14 high grade gliomas (**Table 3**).

All the cases were categorized in three groups according to pathology grade II/III/IV, with Cho/NAA values of 5.36+4.43, 2.59+2.42, and 2.07+1.99 ($P<0.05$), respectively, indicating a significant difference among groups. The means and variances of Cho/NAA ratios were calculated, from which the ROC curve was derived (**Figure 1**). A Cho/NAA cutoff of 2.52 allowed diagnosis of low or high grade pathology; the maximum Youden index was 0.7, and the area under the ROC curve was 0.725 (95% CI: 0.527-0.923). These results were compared to the gold standard with a Cho/NAA cutoff or with subjective judgment according to MRI imaging (**Table 4**). Considering Cho/NAA as 2.52, a significant difference was found between MRS and the conventional MRI scan ($P=0.040$). A typical case is presented in **Figures 2**-**4**, describing a 59-year-old male.

Discussion

Conventional and enhanced MRI can indeed provide important information for many diseases; however, high grade gliomas are easily misdiagnosed as low ones. In this current study, diagnosis sensitivity based on conventional MRI was only 64.3% (**Table 4**), with a considerable fraction of high grade gliomas misdiag-

Table 4. Sensitivity, specificity, misdiagnosis, and diagnosis accordance of MRS and routine MRI, the golden standard of "pathology examination"

Group	Sensitivity	Specificity	NPVs	PPVs	DA
Routine MRI	64.3%	85.7%	54.5%	90.0%	71.4%
MRS	92.9%	71.4%	83.3%	86.7%	85.7%

NPVs: negative predictive values; PPVs: positive predictive values; DA: diagnose accordance.

Figure 2. The Navigus frameless biopsy system with magnetic compatibility fixed in skull (Navigus Medtronic Navigation) was used as puncture appliance in this navigation puncture scene.
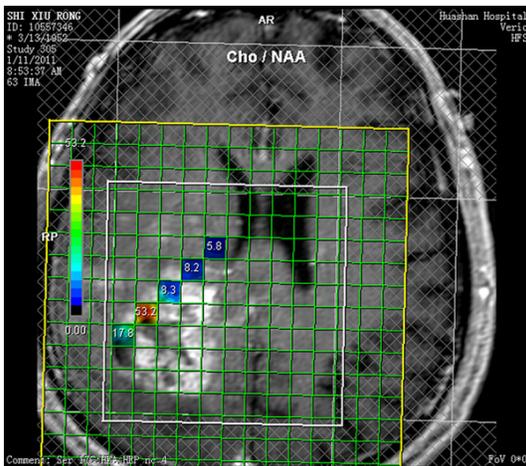
Figure 3. Enormous edema area around the right temporal occipital tumor reveal a slight space-occupying effect. The enhanced lesions are clearly presented as annular enhancement. The puncture target of interest on the MRS metabolic imaging was manually selected, and the puncture properly performed according to the puncture target located in the tumor tissue, near the tumor tissue, and the adjacent tumor tissue.

nosed as low grade. Interestingly, Ginsberg and Elvis et al. [7, 8] showed that lack of enhance-

ment for supratentorial brain tumors in MRI does not imply a low grade tumor [9]. In addition, Christy et al. [10] found that the accuracy of conventional MRI in malignancy grading is only 57%-61%, in line with our results. These findings indicate that conventional MRI cannot provide critical information on tumor physiology such as microvasculature angiogenesis, metabolite changes, and micro-necrosis or cell structure, which is vital for the preoperative grading of brain tumors.

MRS quantitatively and qualitatively analyzes the abnormal metabolism of lesions by detecting concentration changes of certain metabolites in brain tissues, which may correct the flaws of routine CT and MRI imaging. Of note, the chartered property of gliomas on MRS is as follows: significantly increased Cho, significantly decreased NAA, slightly decreased Cr, and increased Lac-Lip peak with the malignancy degree of gliomas. In recent years, MRS has been increasingly used in the preoperative grading of gliomas [11, 12]. Analyzing the accuracy of conventional MRI and MRS, Law and coworkers [13] showed that Cho/Cr and Cho/NAA ratios are relatively appropriate for grading gliomas. NAA was shown to decrease by neuron destruction in tumor tissues, while Cho increased by uncontrolled cell proliferation of tumors, enhancing cell membrane metabolism [14]. Therefore, Cho/NAA ratios increase with the malignancy degree of tumors [15-17]. Our study revealed a significant difference and only a slight overlap of Cho/NAA ratios between low and high grade gliomas, indicating the high sensitivity of Cho/NAA in glioma grading.

In this current study which involved 116 tissue samples from 21 cerebral glioma patients, a significant difference in Cho/NAA between low and high grade gliomas was found, with the Cho/NAA ratio significantly associated with glioma grading (r=0.368, P=0.01), and this result supported the notion that the malignancy degree increases with the Cho/NAA value, in accordance with previous reports [9, 16]. Moreover, we found a Cho/NAA cutoff of 2.52 with the maximum Youden index of 0.7, indicating that MRS, with 92.9% sensitivity, 71.4% specificity, and 85.7% accuracy, is superior to routine plain and enhanced MRI (P=0.040).

Diagnosis accuracy, especially of high grade gliomas, is crucial for treatment and prognosis.
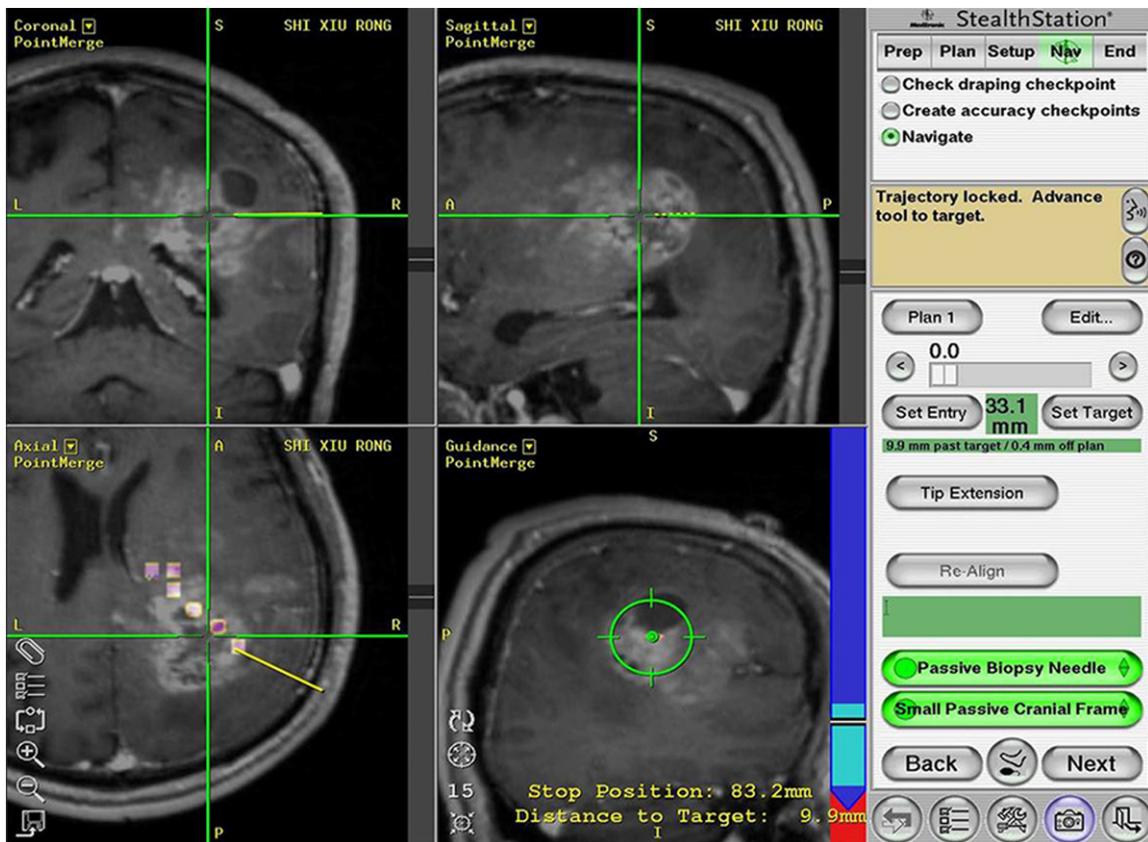
Figure 4. MRS metabolic imaging is effectively and accurately fused with MRI structure imaging by coordinate calculation, and the needle is registered as a navigation bar before sequential biopsy.

Therefore, it is of great importance to identify a threshold value with maximum diagnostic accordance rate for glioma grading and this would need further investigation. Law and et al. [18] set a Cho/NAA threshold value of 0.75, and obtained high grade glioma diagnosis sensitivity and specificity of 96.7 and 10.0%, respectively, suggesting that lower Cho/NAA threshold is more likely to yield higher sensitivity. However, the underlying low specificity may result in excessive medical treatment. Conversely, high specificity may lead to the delay of effective treatment. Consequently, the Cho/NAA value corresponding to the maximum Youden index was selected as cut-off in this study, and although sensitivity and specificity were not favorable, this setting is more effective in distinguishing low and high grade gliomas. Indeed, an improved prediction capacity was achieved with Cho/NAA cutoff of 2.52 (maximum Youden index), in comparison with routine MRI examination. This cut-off value needs further validation in larger sample size studies.

The highlights of this study include: (1) the independently developed marking software Biopsy-NAV, whose accuracy was confirmed by iMRI scan, with a target acquisition rate of 100%; (2) the application of 3.0T MRI to collect body metabolism data of MRS with various voxels may improve image quality, reduce voxel size, ameliorate spatial and spectral resolution, and shorten acquisition time; (3) the effect of brain shift on the material may be effectively avoided by MRS metabolism imaging-guided biopsy before craniotomy.

Nevertheless, some limitations should be noted [18, 19]. ^{1}H-MRS is potentially susceptible to the interference of some portion of the selected ROI close to the skull, cavernous sinus, and cerebral ventricle, which might lead to instable baseline and low spectral imaging quality. In addition, the study adopted a Cho/NAA-based univariate analysis, with Cr and Lip roles in glioma grading not discussed. Furthermore, the obtained results are based on primary clinical experience with a relatively small

sample size; therefore, conclusions should be verified in large sample size studies.

In summary, ^{1}H-MRS as a diagnostic tool, may contribute to accuracy improvement of preoperative glioma grading and needle biopsy [20].

Acknowledgements

Disclosure of conflict of interest

None.

Address correspondence to: Ersong Wang, Department of Neurosurgery, Jinshan Hospital, Fudan University, Shanghai 200433, China. Tel: +86-13817263615; Fax: +86-021-67226910; E-mail: wersong@aliyun.com

References

[1] Filippini G, Falcone C, Boiardi A, Broggi G, Bruzzone MG, Caldiroli D, Farina R, Farinotti M, Fariselli L and Finocchiaro G. Prognostic factors for survival in 676 consecutive patients with newly diagnosed primary glioblastoma. Neuro Oncol 2008; 10: 79-87.

[2] Apuzzo ML, Chandrasoma PT, Cohen D, Zee CS and Zelman V. Computed imaging stereotaxy: experience and perspective related to 500 procedures applied to brain masses. Neurosurgery 1987; 20: 930-937.

[3] Lundsford L. Diagnosis and treatment of brain lesions using the leksell stereotactic system. modern stereotactic neurosurgery. Martinus-Nijhoff, Boston 1989; 145-168.

[4] Graves EE, Nelson SJ, Vigneron DB, Verhey L, McDermott M, Larson D, Chang S, Prados MD and Dillon WP. Serial proton MR spectroscopic imaging of recurrent malignant gliomas after gamma knife radiosurgery. Am J Neuroradiol 2001; 22: 613-624.

[5] Doblas S, He T, Saunders D, Hoyle J, Smith N, Pye Q, Lerner M, Jensen RL and Towner RA. In vivo characterization of several rodent glioma models by 1H MRS. NMR Biomed 2012; 25: 685-694.

[6] Shin JH, Lee HK, Kwun BD, Kim JS, Kang W, Choi CG and Suh DC. Using relative cerebral blood flow and volume to evaluate the histopathologic grade of cerebral gliomas: preliminary results. Am J Roentgenol 2002; 179: 783-789.

[7] Ginsberg LE, Fuller GN, Hashmi M, Leeds NE and Schomer DF. The significance of lack of MR contrast enhancement of supratentorial brain tumors in adults: histopathological evaluation of a series. Surg Neurol 1998; 49: 436-440.

[8] Hermann EJ, Hattingen E, Krauss JK, Marquardt G, Pilatus U, Franz K, Setzer M, Gasser T, Tews DS and Zanella FE. Stereotactic biopsy in gliomas guided by 3-tesla 1H-chemical-shift imaging of choline. Stereotact Funct Neurosurg 2008; 86: 300-307.

[9] Croteau D, Scarpace L, Hearshen D, Gutierrez J, Fisher JL, Rock JP and Mikkelsen T. Correlation between magnetic resonance spectroscopy imaging and image-guided biopsies: semiquantitative and qualitative histopathological analyses of patients with untreated glioma. Neurosurgery 2001; 49: 823-829.

[10] Christy P, Tervonen O, Scheithauer B and Forbes G. Use of a neural network and a multiple regression model to predict histologic grade of astrocytoma from MRI appearances. Neuroradiology 1995; 37: 89-93.

[11] Toyooka M, Kimura H, Uematsu H, Kawamura Y, Takeuchi H and Itoh H. Tissue characterization of glioma by proton magnetic resonance spectroscopy and perfusion-weighted magnetic resonance imaging: glioma grading and histological correlation. Clin Imaging 2008; 32: 251-258.

[12] Kim J, Chang K, Na D, Song I, Kwon B, Han M and Kim K. 3T 1H-MR spectroscopy in grading of cerebral gliomas: comparison of short and intermediate echo time sequences. Am J Neuroradiol 2006; 27: 1412-1418.

[13] Law M, Yang S, Wang H, Babb JS, Johnson G, Cha S, Knopp EA and Zagzag D. Glioma grading: sensitivity, specificity, and predictive values of perfusion MR imaging and proton MR spectroscopic imaging compared with conventional MR imaging. Am J Neuroradiol 2003; 24: 1989-1998.

[14] Tamiya T, Kinoshita K, Ono Y, Matsumoto K, Furuta T and Ohmoto T. Proton magnetic resonance spectroscopy reflects cellular proliferative activity in astrocytomas. Neuroradiology 2000; 42: 333-338.

[15] Wu JS, Zhou LF, Tang WJ, Mao Y, Hu J, Song YY, Hong XN and Du GH. Clinical evaluation and follow-up outcome of diffusion tensor imaging-based functional neuronavigation: a prospective, controlled study in patients with gliomas involving pyramidal tracts. Neurosurgery 2007; 61: 935-948; discussion 948-939.

[16] Stadlbauer A, Gruber S, Nimsky C, Fahlbusch R, Hammen T, Buslei R, Tomandl B, Moser E and Ganslandt O. Preoperative grading of gliomas by using metabolite quantification with high-spatial-resolution proton MR spectroscopic imaging. Radiology 2006; 238: 958-969.

[17] Guo J, Yao C, Chen H, Zhuang D, Tang W, Ren G, Wang Y, Wu J, Huang F and Zhou L. The relationship between Cho/NAA and glioma metabolism: implementation for margin delineation of cerebral gliomas. Acta Neurochir (Wien) 2012; 154: 1361-1370; discussion 1370.

[18] Law M, Yang S, Wang H, Babb JS, Johnson G, Cha S, Knopp EA and Zagzag D. Glioma grading: sensitivity, specificity, and predictive values of perfusion MR imaging and proton MR spectroscopic imaging compared with conventional MR imaging. AJNR Am J Neuroradiol 2003; 24: 1989-1998.

[19] Jackson RJ, Fuller GN, Abi-Said D, Lang FF, Gokaslan ZL, Shi WM, Wildrick DM and Sawaya R. Limitations of stereotactic biopsy in the initial management of gliomas. Neuro Oncol 2001; 3: 193-200.

[20] Law M, Cha S, Knopp EA, Johnson G, Arnett J and Litt AW. High-grade gliomas and solitary metastases: differentiation by using perfusion and proton spectroscopic MR imaging. Radiology 2002; 222: 715-721.